

Journal Pre-proofs

TAT-peptide conjugated repurposing drug against SARS-CoV-2 main protease (3CLpro): potential therapeutic intervention to combat COVID-19

Mohammad Azam Ansari, Qazi Mohammad Sajid Jamal, Suriya Rehman, Ahmad Almatroudi, Mohammad A. Alzohairy, Mohammad N. Alomary, Takshashila Tripathi, Ali H Alharbi, Syed Farooq Adil, Mujeeb Khan, M. Shaheer Malik

PII: S1878-5352(20)30371-3
DOI: <https://doi.org/10.1016/j.arabjc.2020.09.037>
Reference: ARABJC 2829

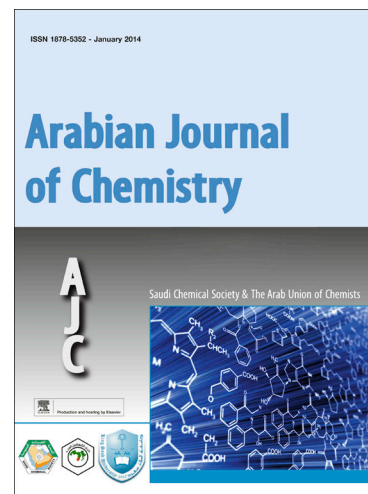
To appear in: *Arabian Journal of Chemistry*

Received Date: 1 July 2020
Revised Date: 19 September 2020
Accepted Date: 21 September 2020

Please cite this article as: M. Azam Ansari, Q. Mohammad Sajid Jamal, S. Rehman, A. Almatroudi, M.A. Alzohairy, M.N. Alomary, T. Tripathi, A.H. Alharbi, S. Farooq Adil, M. Khan, M. Shaheer Malik, TAT-peptide conjugated repurposing drug against SARS-CoV-2 main protease (3CLpro): potential therapeutic intervention to combat COVID-19, *Arabian Journal of Chemistry* (2020), doi: <https://doi.org/10.1016/j.arabjc.2020.09.037>

This is a PDF file of an article that has undergone enhancements after acceptance, such as the addition of a cover page and metadata, and formatting for readability, but it is not yet the definitive version of record. This version will undergo additional copyediting, typesetting and review before it is published in its final form, but we are providing this version to give early visibility of the article. Please note that, during the production process, errors may be discovered which could affect the content, and all legal disclaimers that apply to the journal pertain.

© 2020 Published by Elsevier B.V. on behalf of King Saud University.



1 **TAT-peptide conjugated repurposing drug against SARS-CoV-2 main protease (3CLpro):**
2 **potential therapeutic intervention to combat COVID-19**
3

4 **Mohammad Azam Ansari^{1*}, Qazi Mohammad Sajid Jamal², Suriya Rehman¹, Ahmad**
5 **Almatroudi^{3*}, Mohammad A. Alzohairy³, Mohammad N. Alomary^{4*}, Takshashila Tripathi⁵,**
6 **Ali H Alharbi², Syed Farooq Adil^{6*}, Mujeeb Khan⁶ and M. Shaheer Malik⁷**
7

8 ¹Department of Epidemic Disease Research, Institute for Research & Medical Consultations
9 (IRMC), Imam Abdulrahman Bin Faisal University, P.O. Box 1982, Dammam 31441, Saudi
10 Arabia.

11
12 ²Department of Health Informatics, College of Public Health and Health Informatics, Qassim
13 University, Al Bukayriyah, Saudi Arabia.

14
15 ³Department of Medical Laboratories, College of Applied Medical Sciences, Qassim
16 University, Qassim 51431, Saudi Arabia.

17
18 ⁴National Center for Biotechnology, Life Science and Environmental Research Institute, King
19 Abdulaziz City for Science and Technology, P.O. Box 6086, Riyadh, Saudi Arabia.

20
21 ⁵Department of Neuroscience, Physiology, and Pharmacology, University College London,
22 London, United Kingdom.

23
24 ⁶Department of Chemistry, College of Science, King Saud University, Riyadh 11451, Kingdom
25 of Saudi Arabia.

26
27 ⁷Department of Chemistry, Faculty of Applied Sciences, Umm Al-Qura University, 21955
28 Makkah, Saudi Arabia
29

30 ***Corresponding authors**

31 **Dr. Mohammad Azam Ansari, PhD**

32 Department of Epidemic Disease Research, Institute for Research & Medical Consultations
33 (IRMC), Imam Abdulrahman Bin Faisal University, P.O. Box 1982, Dammam 31441, Saudi
34 Arabia

35 **Email:** maansari@iau.edu.sa
36

37 **Dr. Ahmad Almatroudi, PhD**

38 Department of Medical Laboratories, College of Applied Medical Sciences, Qassim University,
39 Qassim 51431, Saudi Arabia. aamtrody@qu.edu.sa
40

41 **Dr. Mohammad N. Alomary, PhD**

42 National Center for Biotechnology, Life Science and Environmental Research Institute, King
43 Abdulaziz City for Science and Technology, P.O. Box 6086, Riyadh, Saudi Arabia.

44 **Email:** malomary@kacst.edu.sa

45 **Dr. Syed Farooq Adil**

46 Department of Chemistry, College of Science, King Saud University, Riyadh 11451, Kingdom of
47 Saudi Arabia
48 **Email:** sfadil@ksu.edu.sa

49

50

51 **Abstract**

52 The Severe acute respiratory syndrome coronavirus 2 (SARS-CoV-2) that originated in Chinese
53 city of Wuhan has caused around 906,092 deaths and 28,040,853 confirmed cases worldwide
54 (WHO, 11 September, 2020). In a life-threatening situation, where there is no specific and licensed
55 anti-COVID-19 vaccine or medicine available; the repurposed drug might act as a silver bullet.
56 Currently, more than 211 vaccines, 80 antibodies, 31 antiviral drugs, 35 cell-based, 6 RNA-based
57 and 131 other drugs are in clinical trials. It is therefore utter need of the hour to develop an effective
58 drug that can be used for the treatment of COVID-19 before a vaccine can be developed. One of
59 the best-characterized and attractive drug targets among coronaviruses is the main protease
60 (3CL^{pro}). Therefore, the current study focuses on the molecular docking analysis of TAT-peptide⁴⁷⁻
61 ⁵⁷ (GRKKRRQRRRP)-conjugated repurposed drugs (i.e., lopinavir, ritonavir, favipiravir, and
62 hydroxychloroquine) with SARS-CoV-2 main protease (3CL^{pro}) to discover potential efficacy of
63 TAT-peptide (TP) - conjugated repurposing drugs against SARS-CoV-2. The molecular docking
64 results validated that TP-conjugated ritonavir, lopinavir, favipiravir, and hydroxychloroquine have
65 superior and significantly enhanced interactions with the target SARS-CoV-2 main protease. In-
66 silico approach employed in this study suggests that the combination of the drug with TP is an
67 excellent alternative to develop a novel drug for the treatment of SARS-CoV-2 infected patients.
68 The development of TP based delivery of repurposing drugs might be an excellent approach to
69 enhance the efficacy of the existing drugs for the treatment of COVID-19. The predictions from
70 the results obtained provide invaluable information that can be utilized for the choice of candidate
71 drugs for *in vitro*, *in vivo* and clinical trials. The outcome from this work prove crucial for
72 exploring and developing novel cost-effective and biocompatible TP conjugated anti-SARS-CoV-
73 2 therapeutic agents in immediate future.

74 **Keywords:** SARS-CoV-2, TAT-peptide, 3CL^{pro} main protease, COVID-19, *In silico*, Molecular
75 docking, repurposing drug

76

77 **1. Introduction**

78 The Severe acute respiratory syndrome coronavirus 2 (SARS-CoV-2) that originated in Chinese
79 city of Wuhan (Chakraborty et al., 2020a) caused deadly human respiratory infection termed
80 coronavirus disease 2019 (COVID-19) (Huang et al., 2020). World Health Organization (WHO)
81 had declared SARS-CoV-2 a global health emergency on 30th January 2020 (Bhattacharya et al.,
82 2020a) and on 11 March 2020, WHO declared it a pandemic (Rehman et al., 2020). Since the
83 outbreak of COVID-19, as of 11 September 2020, the disease has caused around 906,092 deaths
84 and 28,040,853 confirmed cases of COVID-19 infections worldwide (WHO; 7:08pm CEST, 11
85 September 2020). SARS-CoV-2 belongs to the family *Coronaviruses* and subgenus beta-CoV
86 (Chakraborty et al., 2020b; Saha et al., 2020a). Other previous known coronaviruses that cause
87 severe respiratory diseases in human are MERS-CoV that caused MERS outbreak in the Middle
88 East in 2012 (Chakraborty et al., 2020c) and SARS-CoV caused SARS outbreaks in Guangdong
89 Province, China, in 2006 (Yin et al., 2018). SARS-CoV-2 is single-stranded positive-sense RNA
90 (+ssRNA) virus and the genome size is ~30kb which is the largest among all RNA viruses (Chen
91 et al., 2020; Gralinski and Menachery 2020). SARS-CoV-2 maintains ~80% nucleotide identity
92 with the original SARS-CoV epidemic viruses and 96% with bat coronavirus (Bhattacharya et al.,
93 2020b; Gralinski and Menachery 2020). The genomic sequences of two bat SARS-related CoVs
94 i.e., bat-SL-CoVZC45 and bat-SL-CoVZXC21 showed ~89% sequence similarity with novel
95 SARS-CoV-2. Phylogenetic analysis has indicated that the SARS-CoV-2 is a viral recombinant of
96 previously identified bat coronaviruses (Ansari et al., 2020; Chan et al., 2020).

97 The repurposing antiretroviral protease inhibitor drugs such as lopinavir/ritonavir, indinavir,
98 saquinavir and antiviral RNA polymerase inhibitors drug such as remdesivir are currently being
99 tested for the treatment of SARS-CoV-2 (Paules et al., 2020; Li et al., 2020; Liu et al., 2020).
100 Recently, antiviral efficacy of remdesivir and chloroquine against SARS-CoV-2 clinical isolate
101 has been investigated and was found that they can potentially inhibit SARS-CoV-2 at the low-
102 micromolar concentration *in vitro* (Holshue et al., 2020; Wang et al., 2020). Nafamostat,
103 Nitazoxanide, Ribavirin, Penciclovir and Favipiravir are other drugs that have been tested against
104 SARS-CoV-2 also show potential inhibitory effects *in vitro* (Wang et al., 2020).

105 Currently, no vaccine or medicine has been developed that can be used for the treatment of SARS-
106 CoV-2 infections, therefore, the repurposed drug could act as a brilliant alternative with potential
107 to combat the disease effectively (Saha et al., 2020b). Though, preclinical and clinical trials are
108 required to ensure their effectiveness, such treatment might be better and promising than a placebo.

109 A number of clinical trials are being done to test the efficacy of protease inhibitors drugs lopinavir
110 and ritonavir against SARS-CoV-2. These drugs are commonly used in the treatment of HIV
111 infections. The combination of lopinavir and ritonavir with Chinese herbal medicines was used in
112 preliminary clinical studies for the treatment of SARS-CoV-2 (Wang et al., 2020). In vitro studies
113 show that hydroxychloroquine and chloroquine have potential anti-COVID-19 activity (Gautret et
114 al., 2020; Gao et al., 2020). According to Milken Institute, 211 vaccines, 31 antiviral drugs, 35
115 cell-based, 80 antibodies, 6 RNA-based and 131 others drugs are at different phases of
116 development and trials (<https://milken-institute-covid-19-tracker.webflow.io/>). It is therefore dire
117 need to develop an effective drug that can be used for the treatment of COVID-19 before a vaccine
118 can be developed.

119 Moreover, the efficiency of these potential anti-COVID drugs can be further enhanced by
120 combining them with cell-penetrating peptides (CPPs), which can possibly help to enhance the
121 cellular uptake of these drugs (Nori et al., 2003). CPPs are short peptides (less than 30 residues)
122 consisting of excellent capability to cross cellular membranes with very limited toxicity, via
123 energy-dependent and/or independent mechanisms, without the necessity of a chiral recognition
124 by specific receptors (Bechara and Sagan 2003; Ansari et al., 2020). The main antiviral approach
125 of CPPs has been the conjugation of CPPs with potential drug molecules; however, some CPPs
126 have even demonstrated antiviral properties by themselves (Pärn et al., 2015).

127 The cell-penetrating ability of TAT-peptide (TP) commenced a new era in intracellular drug
128 delivery. TAT-peptide⁴⁷⁻⁵⁷ (GRKKRRQRRRP), a short cation richer with basic amino acid peptide
129 is commonly used as research tool to enhance the delivery and transport of drugs, DNA, RNA,
130 proteins, viruses and nanoparticles inside the cytoplasm (Quan et al., 2019; Skwarczynski and Toth
131 2019; Ansari et al., 2020). We have suggested that the efficacy of antiviral activity of these
132 repurposing drugs against COVID-19 can be improved and enhanced by conjugating it to the TP.
133 Therefore, the current study focuses on the molecular docking analysis of TP (GRKKRRQRRRP)-
134 conjugated repurposed drugs (lopinavir, ritonavir, favipiravir, and hydroxychloroquine) with
135 SARS-CoV-2 main protease (3CL hydrolase, PDB: 6LU7) to discover potential efficacy of TP-
136 conjugated repurposed drugs against SARS-CoV-2.

137

138 **2. Methodology**

139 **2.1 Receptor molecule preparation**

140 The crystal structure of COVID-19 main protease is complex with an inhibitor N3 (PDB ID: 6LU7)
141 downloaded from Protein Data Bank (PDB), a well-known 3 Dimensional bio-macromolecular
142 repository (**Figure 1**). The 3D structure was developed by X-Ray diffraction method with the
143 observed resolution of 2.16 Å, R-Value Free 0.235, R-Value Work 0.202, and R-Value
144 observed 0.204 (PDB ID: 6LU7). N3 inhibitor, HETATOM, and water molecules were removed
145 from the 3D structure PDB file (PDB ID: 6LU7). Active site amino acid residues (Asn142,
146 Cys145, Gln189, Glu166, Gly143, His163, His164, Met165, Phe140, Thr190, Thr26) information
147 of N3 inhibitor interaction with 6LU7 has been obtained for the docking analysis of selected drug
148 molecules on same active site. After that CHARMM force field was applied on PDB ID: 6LU7
149 3D structure for the energy minimization process. Discovery Studio visualizer 2019 was used for
150 afore mentioned editing of 3D structure.

151 **2.3 3D structure modeling of TAT-Peptide**

152 TAT-peptide (GRKKRRQRRRP) an 11 amino acid residue, rich in basic amino acid derived from
153 nuclear transcription activator tat protein of human immunodeficiency virus-1 which penetrates
154 various cell types (Fang et al., 2013) was submitted to PEP-FOLD3.5 webserver to generate the
155 3D structure of TP (Lamiable et al., 2016). PEP-FOLD3 server used the Hidden Markov Model
156 sub-optimal conformation sampling approach for the prediction of the 3D structure of small
157 peptide.

158 **2.4 TAT-Peptide 3D structure validation**

159 After successful generation of TP modeled, 3D structure was further assessed by MolProbit tool
160 (Chenn et al., 2010) integrated in structure assessment module of SwissModel server (Waterhouse
161 et al 2018).

162 **2.5 Preparation of Drug Molecules**

163 The performance of repurposed drugs Lopinavir, Ritonavir, Favipiravir, and Hydroxychloroquine
164 with and without TP was explored to perform in silico interaction analysis with COVID-19
165 Protease (PDB ID: 6LU7). The chemical canonical SMILES IDs of selected drugs were extracted
166 from PubChem Database (<https://pubchem.ncbi.nlm.nih.gov/>). Furthermore, we have generated a
167 3D structure of drug molecules using CORINA classic 3D structure generator server
168 (https://www.mn-am.com/online_demos/corina_demo) (**Table 1**). Also discovery studio 2019

169 was used to implement the CHARMM force field in order to complete the energy minimization
170 process for the generated 3D structures of drug molecules (Vanommeslaeghe et al. 2010). Apart
171 from these, it has been suggested that nanotechnology could be an alternative therapeutic approach
172 that can be used to counter COVID-19 and similar pandemics (Weiss et al., 2020; Gaurav et al.,
173 2020).

174 **2.6 In silico molecular Interaction Analysis**

175 The in silico interaction analysis was executed into two parts:

176 **2.6.1. Molecular docking of repurposed drugs without TAT-peptide with COVID-19 main** 177 **protease**

178 The docking experimentation between free drug (without TAT-peptide) and COVID-19 protease
179 (PDB ID: 6LU7) was executed with the help of AutoDock 4.2 MGL tools version 1.5.6. AutoDock
180 uses a Lamarckian Genetic Algorithm and empirical binding free energy function as a scoring
181 function for the ligand-receptor interaction (Morris et al., 1998). The docking was performed on the
182 active site after implementing the default AutoDock parameters. However, to cover the maximum
183 area within the grid box 60x60x60 Å which can accommodate the selected active site residues in
184 the grid box, the grid center point coordinates X, Y and Z were set as -15.217, 14.435 and 60.367,
185 respectively with the default value of grid points spacing 0.375 Å.

186 **2.6.2. Molecular docking of TAT-Peptide-conjugated repurposed drug with COVID-19 main** 187 **protease**

188 AutoDock 4.2 tool was used to prepare TAT-Peptide-conjugated drug complexes. After that TAT-
189 Peptide-conjugated drug complexes were docked with COVID-19 protease (PDB ID: 6LU7) using
190 the PatchDock online docking server (<https://bioinfo3d.cs.tau.ac.il/PatchDock/>). PatchDock uses
191 a geometry-based molecular docking algorithm as a scoring function (Schneidman-Duhovny et al.,
192 2005). After performing docking analysis, results were analyzed and 3D graphics was generated
193 using discovery Studio Visualizer, 2019.

194

195 **2.4 Results and Discussion**

196 Currently, 548 unique therapeutic compounds are in development and 176 of those are in the
197 clinical stage i.e., 26 in phase I, 86 in phase II, 41 in phase III and 23 are in phase IV
198 (<https://www.bio.org/policy/human-health/vaccines-biodefense/coronavirus/pipeline-tracker>).

199 Among them, repurposed drugs such as remdesivir, lopinavir, ritonavir, favipiravir, and
200 hydroxychloroquine show great therapeutic potential in the prevention and treatment of COVID-
201 19 infections. However, the discovery of the cell-penetrating function of HIV1-TAT protein in
202 1988 quickly became a popular research tool used to enhance the intracellular delivery and
203 transport of drugs and a large number of biomolecules (Skwarczynski and Toth 2019). Thus, to
204 improve the efficacy of repurposed drugs, CPPs can be conjugated to drug or formulation. CPPs
205 can deliver drugs directly to the cytoplasm either by endocytic or nonendocytic pathways. At
206 present, a large number of naturally derived as well as synthetic or artificial CPPs have been
207 characterized and used for the intracellular delivery of a variety of cargos such as small molecules,
208 drugs, DNA/RNA, peptide, proteins, liposomes and nanoparticles into cells (Skwarczynski and
209 Toth 2019). CPPs are also easy to prepare, cost-effective, and most importantly, they are usually
210 non-toxic (Skwarczynski and Toth 2019). It has been investigated that HIV1 TP directly penetrate
211 the membranes by generating nanoscale pores (Ciobanasi et al., 2010). The preclinical and clinical
212 trials on cancer diagnosis and treatment show that CPP-based drug delivery systems enhance the
213 efficiency of the delivery of anti-cancer drugs and imaging reagents (Tripathi et al., 2018). Thus,
214 the development of CPP-based delivery of repurposing drugs might be an excellent approach to
215 enhance the efficacy of the existing drugs for the treatment of COVID-19.

216 One of the best-characterized and attractive drug targets among coronaviruses is the main protease
217 (3CL^{pro}) (Anand et al., 2003; Hang et al., 2020). Along with the papain-like protease(s), this
218 enzyme is essential for processing the polyproteins that are translated from the viral RNA
219 (Hilgenfeld 2014). The 3CL protease of coronaviruses facilitates viral assembly by cleaving
220 almost 11 sites on the large polyproteins. Inhibiting the activity of the protease enzyme would
221 block viral replication and also prevent the progression of the disease (Hilgenfeld 2014). The
222 protein sequences of COVID-19 Main protease (2019-nCoV Mpro) and SARS-CoV Mpro are 96%
223 identical (Bhattacharya et al., 2020b). In several studies, the similarities in the sequence of a
224 potential target for COVID-19 to that of the SARS Mpro were utilized to build a model for the
225 structure of SARS-CoV-2 Mpro. Homology based models were utilized to screen a library of

226 compounds to predict potential drugs for COVID-19 (Nguyen et al., 2020; Xu et al., 2020; Liu et
227 al., 2020).

228 The availability of the high-resolution X-ray crystal structures of the target i.e., the main protease
229 of SARS-CoV-2 Mpro (PDB ID: 6LU7), has been utilized in the current study as the target for
230 molecular docking based virtual screening of TP-conjugated repurposing antiretroviral, antiviral
231 and antimalarial drugs. The 3D modelled structure of TP used in this study was generated by PEP-
232 FOLD3.5 (**Figure 2**). Further, the 3D modeled structure of TP was validated by MolProbity tool
233 integrated in structure assessment module of SwissModel server. It was observed that number of
234 residues found in the favored region was ~100.0% and no residues were found in Ramachandran
235 Outliers and Rotamer Outliers regions (**Figure 3A**). The MolProbity Score was 0.50 and
236 QMEAN4 score was less than <1 as compared with standard ideal value that should be between
237 0-1 for good quality predicted structure (Benkert et al., 2011) (**Figure 3B**). So, 3D structure of TP
238 was found to be acceptable in order to perform further *in silico* interaction analysis. For the first
239 time, TP was conjugated with lopinavir, ritonavir, favipiravir and hydroxychloroquine using
240 AutoDock tool to investigate their binding affinity and interaction with COVID-19 main protease.
241 The 3D structure of individual drug with TP to perform in silico analysis with COVID-19 Protease
242 was shown in **Table 1**. AutoDock analysis was also performed to illustrate the possible interaction
243 between TP and drugs. The interaction between TP and drugs shows that a number of several
244 others types of molecular contacts were also involved apart from hydrogen bonds that provide
245 more stability to the complex. During Ritonavir and TP interaction Arg,3 Lys4, Lys5, Arg6, Arg7
246 and Gln8 were also involved in Alkyl and Pi-Alkyl bonding apart from conventional hydrogen
247 bond and van der walls interactions (**Figure 4C**). During Lopinavir and TP interaction Lys4, Arg6
248 and Arg9 were involved in Alkyl and Pi-Alkyl interaction apart from hydrogen bond, carbon-
249 hydrogen bond and van der walls interactions (**Figure 5C**). Favipiravir and TP interaction shows
250 Pi-Sigma contact, hydrogen bond and van der Walls interaction (**Figure 6C**). In case of
251 hydroxychloroquine and TP interaction Tyr1, Lys4, Lys5 and Arg9 were involved in Alkyl and
252 Pi-Alkyl bonding apart from hydrogen bond, carbon-hydrogen bond and van der walls interactions
253 (**Figure 7C**).

254 We postulated that after conjugating repurposed drug to TAT-peptide, the binding affinity was
255 enhanced to counter the COVID-19 protease. Further, it was also hypothesized that the TP

256 conjugated repurposing drugs interact more strongly and efficiently than drugs without TAT
257 conjugate. In the present study, the obtained results support our experimental hypothesis. The
258 molecular docking study showed that the interaction of repurposed drugs ritonavir, lopinavir,
259 favipiravir and hydroxychloroquine (without TP conjugation) formed 5, 4, 8 and 2 H-bonds,
260 respectively, when docked with COVID-19 main protease (**Table S1, S3; Fig 4ab, 5ab,6ab, 7ab**).
261 The visualization of full 3D structures of COVID-19 main protease docked with the individual
262 drugs without TP was shown in supplementary figure (**S1-S5**). The observed binding energy score
263 was -9.16 kcal/mol for ritonavir, -7.57 kcal/mol for lopinavir, -4.23 kcal/mol for favipiravir and -
264 6.61 kcal/mol for hydroxychloroquine (**Table S1**). The results of molecular docking for
265 compounds currently in clinical trials predict that ritonavir and lopinavir are in Phase IV of clinical
266 trials, has the best binding energy for inhibition of Mpro of SARS-CoV-2 (-9.16 and -7.57
267 kcal/mol, **Table S1**). The favipiravir, an antiviral drug that inhibits viral RNA-dependent RNA-
268 polymerase is currently in Phase 2, 3 and 4 for treatment of COVID-19, has the binding energy for
269 inhibition of Mpro of SARS-CoV-2 (i.e., -4.23 kcal/mol, **Table S1**) are weaker binders than
270 ritonavir & lopinavir (-9.16 & -7.57 kcal/mol). Lopinavir and ritonavir have been reported in
271 earlier studies as potential drug candidates that target Mpro of SARS-CoV-2. In this study, the
272 binding energies for ritonavir and lopinavir (-9.16 & -7.57 kcal/mol) are in good agreement with
273 previous molecular docking study (Sekhar 2020) and are consistent with preliminary clinical data
274 indicating effectiveness for these drugs (Wang et al., 2020). Hydroxychloroquine, an antimalarial
275 drug has been found to be efficient on SARS-CoV-2 and reported to be beneficial in Chinese COV-
276 19 patients (Gautret et al., 2020). Hydroxychloroquine has been approved for human clinical trials
277 and currently in Phase I, II, III and IV for treatment of COVID-19, has the binding energy of -6.61
278 kcal/mol (**Table S1**), indicating a potential for increased efficacy. Based on the modeled structure
279 of SARS-CoV-2 (Mpro), molecular docking and free energy, it was predicted that ritonavir,
280 lopinavir, and hydroxychloroquine are the most potent drug candidates for COVID-19. In contrary
281 to the drug without TP-conjugation, the molecular docking study of TP-conjugated ritonavir,
282 lopinavir, favipiravir and hydroxychloroquine complex showed enhanced binding affinity with
283 COVID-19 Main protease (**Figure 4D,5D,6D,7D; Table S2**). It has been observed that the efficacy
284 of repurposed drugs have been enhanced after conjugating with TP when compared to drug without
285 TP. When TP was interacted with ritonavir, lopinavir, favipiravir, and hydroxychloroquine only 4,
286 1, 3, and 2 H-bond were formed (**Table S3**). However, when TP-conjugated ritonavir, lopinavir,

287 favipiravir, and hydroxychloroquine drug complex were docked with COVID-19 main protease 8,
288 10, 10, and 15 H-bonds were formed which are comparatively much higher than that of the drug
289 without the TP (**Figure 4D,5D,6D,7D; Table S2, S3**). After comparing the molecular docking
290 data of drugs without TP with COVID-19 protease (**Figure 4ab, 5ab, 6ab,7ab; Table S1**) and TP-
291 conjugated drug complex (**Figure 4D,5D,6D,7D; Table S2**), it has been found that TP- conjugated
292 drugs interacted most efficiently with COVID-19 main protease (**Table S3**). The molecular
293 docking results revealed and validated that TP-conjugated drugs have superior and significantly
294 enhanced interaction with the target SARS-CoV-2 Main protease (**Table S2, S3**). The results of
295 the current study confirm the therapeutic potential of TP-conjugated drugs complex against SARS-
296 CoV-2 Mpro; therefore, these TP-conjugated drug complexes are reassuring and more suitable for
297 therapeutic application of COVID-19 treatment than the existing free drugs. Further, the
298 therapeutic potential TP-conjugated repurposed drugs can be enhanced and improved by utilizing
299 various nanomedicine-based drug delivery approaches e.g., lipid-based nanoparticles (solid lipid
300 nanoparticle, nanoemulsion, liposome), polymeric nanoparticles (poly lactic-co-glycolic acid, poly
301 ϵ -caprolactone), dendrimers, polymeric micelles etc [Ansari et al., 2020]. Nanomedicine-based
302 delivery techniques possibly augment the efficacy of the drugs by facilitating controlled-release
303 and may also enhance the bioavailability and reduce side effects [Lembo et al., 2018]. The
304 manufactured nanocarriers may easily get to specific extracellular /intracellular targets site and
305 thus can compete with virus for their attachment to the cell surface receptors [Lembo et al., 2018].
306 As a result, nanomedicine based-drug delivery approach is promising alternative strategies that
307 can be explored to develop the broad-spectrum antiviral drugs against current COVID-19 infection
308 [Lembo et al., 2018]. Moreover, organometallic complexes and nanocomposites can also be
309 evaluated for anti-SARS-CoV-2 therapeutic agents. However, further extensive research is
310 required before these nanomedicines based TP-conjugated drugs will be ready for advanced
311 clinical trials.

312

313

314 **Conclusion**

315 CPPs are promising immune enhancers when incorporated into appropriate drug delivery systems.

316 CPPs has a number of advantages over other translocation and delivery methods as it is easy to

317 prepare, inexpensive and normally have low cell toxicity with no immunological response. Drug
318 development against SARS-CoV-2 is considered urgent in order to fight COVID-19. The present
319 study suggests that TP-conjugated drugs will be effective in treating COVID-19. The molecular
320 docking results validated that TP-conjugated ritonavir, lopinavir, favipiravir, and
321 hydroxychloroquine have superior and significantly enhanced interactions with the target SARS-
322 CoV-2 Main protease (Mpro). TAT-peptide has a higher capability to translocate into a wide range
323 of cell types, higher rate of cellular permeability and uptake, easier to pass through other biological
324 barriers. In conclusion, in-silico approach employed in this study suggests that the combination of
325 the drug with TP is an excelling alternative to develop a novel drug for the treatment of SARS-
326 CoV-2 infected patients. The predictions from the results obtained provide invaluable information
327 that can be utilized for the choice of candidate drugs for *in vitro*, *in vivo* and clinical trials. The
328 outcomes from this work prove crucial for exploring and developing novel cost-effective and
329 biocompatible TP-conjugated anti-SARS-CoV-2 therapeutic agents in immediate future.

330 **Funding:** Deanship of Scientific Research, Imam Abdulrahman Bin Faisal University, Dammam,
331 Saudi Arabia, Grant number-Covid19-2020-002-IRMC.
332

333 References

- 334 Anand, K., Ziebuhr, J., Wadhwani, P., Mesters, J.R., Hilgenfeld, R., 2003. Coronavirus main
335 proteinase (3CLpro) structure: Basis for design of anti-SARS drugs. *Science*. 300, 1763–1767.
336
- 337 Ansari, M.A., Almatroudi, A., Alzohairy, M.A., AlYahya, S., Alomary, M.N., Al-Dossary, H.A.,
338 Alghamdi, S., 2020. Lipid-based nano delivery of Tat-peptide conjugated drug or vaccine-
339 promising therapeutic strategy for SARS-CoV-2 treatment. *Expert Opinion on Drug Delivery*. 31,
340 1-4
341
- 342 Bechara, C., Sagan, S., 2013. Cell-penetrating peptides: 20 years later, where do we stand?. *FEBS*
343 *letters*, 587, 1693-1702.
344
- 345 Benkert, P., Biasini, M., Schwede, T., 2011. Toward the estimation of the absolute quality of
346 individual protein structure models. *Bioinformatics*. 27, 343-350.
347
- 348 Bhattacharya, M., Sharma, A.R., Patra, P., Ghosh, P., Sharma, G., Patra, B.C., Saha, R.P., Lee,
349 S.S., Chakraborty, C., 2020a. A SARS-CoV-2 vaccine candidate: In-silico cloning and validation.
350 *Informatics in Medicine Unlocked*. 20,100394.
351
- 352 Bhattacharya, M., Sharma, A.R., Patra, P., Ghosh, P., Sharma, G., Patra, B.C., Lee, S.S.,
353 Chakraborty, C., 2020b. Development of epitope-based peptide vaccine against novel coronavirus
354 2019 (SARS-COV-2): Immunoinformatics approach. *Journal of Medical Virology*. 92, 618-631.

- 355
356 Chakraborty, C., Sharma, A.R., Sharma, G., Bhattacharya, M., Lee, S.S., 2020a. SARS-CoV-2
357 causing pneumonia-associated respiratory disorder (COVID-19): diagnostic and proposed
358 therapeutic options. *Eur Rev Med Pharmacol Sci.* 24, 4016-4026.
359
- 360 Chakraborty, C., Sharma, A.R., Bhattacharya, M., Sharma, G., Lee, S.S., 2020b. The 2019 novel
361 coronavirus disease (COVID-19) pandemic: A zoonotic prospective. *Asian Pacific Journal of*
362 *Tropical Medicine.* 13, 242-246.
363
- 364 Chakraborty, C., Sharma, A.R., Sharma, G., Bhattacharya, M., Saha, R.P., Lee, S.S., 2020.
365 Extensive Partnership, Collaboration, and Teamwork is Required to Stop the COVID-19 Outbreak.
366 *Archives of Medical Research.* <https://doi.org/10.1016/j.arcmed.2020.05.021>
367
- 368 Chan, J.F.W., Kok, K.H., Zhu, Z., Chu, H., To, K.K.W., Yuan, S., Yuen, K.Y., 2020. Genomic
369 characterization of the 2019 novel human-pathogenic coronavirus isolated from a patient with
370 atypical pneumonia after visiting Wuhan. *Emerg. Microbes Infect.* 9, 221-36.
371
- 372 Chen, Y., Liu, Q., Guo, D., 2020. Emerging coronaviruses: genome structure, replication, and
373 pathogenesis. *J Medical Virol.* 92, 18-23.
374
- 375 Chenn V.B., Arendall W.B., Headd J.J., Keedy D.A., Immormino R.M., Kapral G.J., Murray L.W.,
376 Richardson J.S., Richardson D.C., 2010. All-atom structure validation for macromolecular
377 crystallography. *Acta Cryst.* D66, 16-21.
378
- 379 Ciobanasu, C., Siebrasse, J.P., Kubitscheck, U., 2010. Cell-penetrating HIV1 TAT peptides can
380 generate pores in model membranes. *Biophysical J.* 7,153-62.
- 381 Fang, S.L., Fan, T.C., Fu, H.W., Chen, C.J., Hwang, C.S., Hung, T.J., Lin, L.Y., Chang, M.D.T.,
382 2013. A novel cell-penetrating peptide derived from human eosinophil cationic protein. *PloS one.*
383 8, e57318.
384
- 385 Gao, J., Tian, Z., Yang, X., 2020. Breakthrough: Chloroquine phosphate has shown apparent
386 efficacy in treatment of COVID-19 associated pneumonia in clinical studies. *Bioscience Trends.*
387 14, 72-73.
388
- 389 Gaurav, C., Marc, J.M., Sourav, K., Vianni, C., Deepa, G., Sergio, O., 2020. Nanotechnology for
390 COVID-19: Therapeutics and Vaccine Research. *ACS Nano.*
391 <https://doi.org/10.1021/acsnano.0c04006>
- 392 Gautret, P., Lagier, J.C., Parola, P., Meddeb, L., Mailhe, M., Doudier, B., Courjon, J.,
393 Giordanengo, V., Vieira, V.E., Dupont, H.T., Honoré, S., 2020. Hydroxychloroquine and
394 azithromycin as a treatment of COVID-19: results of an open-label non-randomized clinical trial.
395 *International J Antimicrobial agents.* 105949.
396
- 397 Gralinski, L.E., Menachery, V.D., 2020. Return of the Coronavirus: 2019-nCoV. *Viruses.* 12, 135.
398

- 399 Hang, L., Lin, D., Sun, X., Curth, U., Drosten, C., Sauerhering, L., Becker, S., Rox, K., Hilgenfeld,
400 R., 2020. Crystal structure of SARS-CoV-2 main protease provides a basis for design of improved
401 α -ketoamide inhibitors. *Science*. 368, 409-412.
- 402
- 403 Hilgenfeld, R., 2014. From SARS to MERS: Crystallographic studies on coronaviral proteases
404 enable antiviral drug design. *FEBS J*. 281, 4085–4096.
- 405
- 406 Holshue, M.L., DeBolt, C., Lindquist, S., Lofy, K.H., Wiesman, J., Bruce, H., Spitters, C., Ericson,
407 K., Wilkerson, S., Tural, A., Diaz, G., 2020. First case of 2019 novel coronavirus in the United
408 States. *N Engl J Med*. 382, 929-936.
- 409
- 410 **<https://milken-institute-covid-19-tracker.webflow.io/>** LAST UPDATED:SEPTEMBER 10, 2020
411 8:26 AMPACIFIC
- 412
- 413 **<https://www.bio.org/policy/human-health/vaccines-biodefense/coronavirus/pipeline-tracker>**
- 414
- 415 **<https://covid19.who.int/>** Updated: September 11, 2020, 7:08pm CEST
- 416
- 417 Huang, C., Wang, Y., Li, X., Ren, L., Zhao, J., Hu, Y., Zhang, L., Fan, G., Xu, J., Gu, X., Cheng,
418 Z., 2020. Clinical features of patients infected with 2019 novel coronavirus in Wuhan, China. *The*
419 *lancet*, 395,497-506.
- 420
- 421 Lamiable, A., Thévenet, P., Rey, J., Vavrusa, M., Derreumaux, P., Tufféry, P., 2016. PEP-FOLD3:
422 faster de novo structure prediction for linear peptides in solution and in complex. *Nucleic Acids*
423 *Res*. 44, W449–W454. ([https://mobyle.rpbs.univ-paris-diderot.fr/cgi-bin/portal.py#forms::PEP-](https://mobyle.rpbs.univ-paris-diderot.fr/cgi-bin/portal.py#forms::PEP-FOLD3)
424 [FOLD3](https://mobyle.rpbs.univ-paris-diderot.fr/cgi-bin/portal.py#forms::PEP-FOLD3))
- 425
- 426 Lembo, D., Donalisio, M., Civra, A., Argenziano, M., Cavalli, R., 2018. Nanomedicine
427 formulations for the delivery of antiviral drugs: a promising solution for the treatment of viral
428 infections. *Expert Opin Drug Deliv*, 15:93-114.
- 429
- 430 Li, G., De Clercq, E., 2020. Therapeutic options for the 2019 novel coronavirus (2019-nCoV).
431 *Nature Reviews Drug Discovery*. 19, 149-150.
- 432
- 433 Liu, W., Morse, J.S., Lalonde, T., Xu, S., 2020. Learning from the past: possible urgent prevention
434 and treatment options for severe acute respiratory infections caused by 2019-nCoV.
435 *Chembiochem*. <https://doi.org/10.1002/cbic.202000047>
- 436
- 437 Liu, X., Wang, X.J., 2020. Potential inhibitors against 2019-nCoV coronavirus M protease from
438 clinically approved medicines. *Journal of Genetics and Genomics*. 47, 119.
- 439
- 440 Lovell, S.C., Davis, I.W., Arendall III, W.B., De Bakker, P.I., Word, J.M., Prisant, M.G.,
441 Richardson, J.S., Richardson, D.C., 2003. Structure validation by $C\alpha$ geometry: ϕ , ψ and $C\beta$
442 deviation. *Proteins: Structure, Function, and Bioinformatics*. 50, 437-50.

- 443
444 Morris, G.M., Goodsell, D.S., Halliday, R.S., Huey, R., Hart, W.E., Belew, R.K., Olson, A.J.,
445 1998. Automate Docking Using a Lamarckian Genetic Algorithm and an Empirical Binding
446 Free Energy Function *J. Computational Chemistry*, 1998; 19:1639-1662.
- 447
448 Nguyen, D., Gao, K., Chen, J., Wang, R., Wei, G., 2020. Potentially highly potent drugs for 2019-
449 nCoV. bioRxiv. doi: <https://doi.org/10.1101/2020.02.05.936013>
- 450
451 Nori, A., Jensen, K.D., Tijerina, M., Kopecková, P., Kopeček, J., 2003. Tat-conjugated synthetic
452 macromolecules facilitate cytoplasmic drug delivery to human ovarian carcinoma cells.
453 *Bioconjugate Chem.* 14, 44-50.
- 454
455 Pärn, K., Eriste, E., Langel, Ü., 2015. The antimicrobial and antiviral applications of cell-
456 penetrating peptides. In *Cell-Penetrating Peptides* (pp. 223-245). Humana Press, New York, NY.
- 457
458 Paules, C.I., Marston, H.D., Fauci, A.S., 2020. Coronavirus infections—more than just the
459 common cold. *JAMA.* 323, 707-8.
- 460
461 Quan, X., Sun, D., Zhou, J., 2019. Molecular mechanism of HIV-1 TAT peptide and its conjugated
462 gold nanoparticles translocating across lipid membranes. *Physical Chemistry Chemical Physics.*
463 21, 10300-10.
- 464
465 Rehman, S., Majeed, T., Ansari, M.A., Ali, U., Sabit, H., Al-Suhaimi, E.A., 2020. Current scenario
466 of COVID-19 in pediatric age group and physiology of immune and thymus response. *Saudi
Journal of Biological Sciences.* <https://dx.doi.org/10.1016%2Fj.sjbs.2020.05.024>
- 467
468 Saha, A., Sharma, A.R., Bhattacharya, M., Sharma, G., Lee, S.S., Chakraborty, C., 2020a.
469 Tocilizumab: A therapeutic option for the treatment of cytokine storm syndrome in COVID-19.
Archives of Medical Research. 51, 595-597.
- 470
471 Saha, A., Sharma, A.R., Bhattacharya, M., Sharma, G., Lee, S.S., Chakraborty, C., 2020b.
472 Probable Molecular Mechanism of Remdesivir for the Treatment of COVID-19: Need to Know
More. *Archives of Medical Research.* 51, 585-586.
- 473
474 Schneidman-Duhovny, D., Inbar, Y., Nussinov, R., Wolfson, H.J., 2005. PatchDock and
475 SymmDock: servers for rigid and symmetric docking. *Nucl. Acids. Res.* 33, W363-367.
- 476
477 Sekhar, T., 2020. Virtual Screening based prediction of potential drugs for COVID-19.
478 doi:10.20944/preprints202002.0418.v2. Preprints (www.preprints.org)
- 479
480 Skwarczynski, M., Toth, I., 2019. Cell-penetrating peptides in vaccine delivery: facts, challenges
481 and perspectives. *Ther. Deliv.* 10, 465-467.
- 482
483 Tripathi, P.P., Arami, H., Banga, I., Gupta, J., Gandhi, S., 2018. Cell penetrating peptides in
preclinical and clinical cancer diagnosis and therapy. *Oncotarget.* 9, 37252-37267.

484
485 Vanommeslaeghe, K., Hatcher, E., Acharya, C., Kundu, S., Zhong, S., Shim, J., Darian, E.,
486 Guvench, O., Lopes, P., Vorobyov, I., Mackerell Jr, A.D., 2010. CHARMM general force field: A
487 force field for drug-like molecules compatible with the CHARMM all-atom additive biological
488 force fields. *Journal of computational Chemistry*. 31, 671-90.

489 Wang, M., Cao, R., Zhang, L., Yang, X., Liu, J., Xu, M., Shi, Z., Hu, Z., Zhong, W., Xiao, G.,
490 2020. Remdesivir and chloroquine effectively inhibit the recently emerged novel coronavirus
491 (2019-nCoV) in vitro. *Cell Res*. 30, 269-71.

492
493 Wang, Z., Chen, X., Lu, Y., Chen, F., Zhang, W., 2020. Clinical characteristics and therapeutic
494 procedure for four cases with 2019 novel coronavirus pneumonia receiving combined Chinese and
495 Western medicine treatment. *Bioscience Trends*. 14, 64-68.

496
497 Weiss, C., Carriere, M., Fusco, L., Capua, I., Regla-Nava, J.A., Pasquali, M., Scott, J.A., Vitale,
498 F., Unal, M.A., Mattevi, C., Bedognetti, D., 2020. Toward Nanotechnology-Enabled Approaches
499 against the COVID-19 Pandemic. *ACS Nano*. 14, 6, 6383–6406.

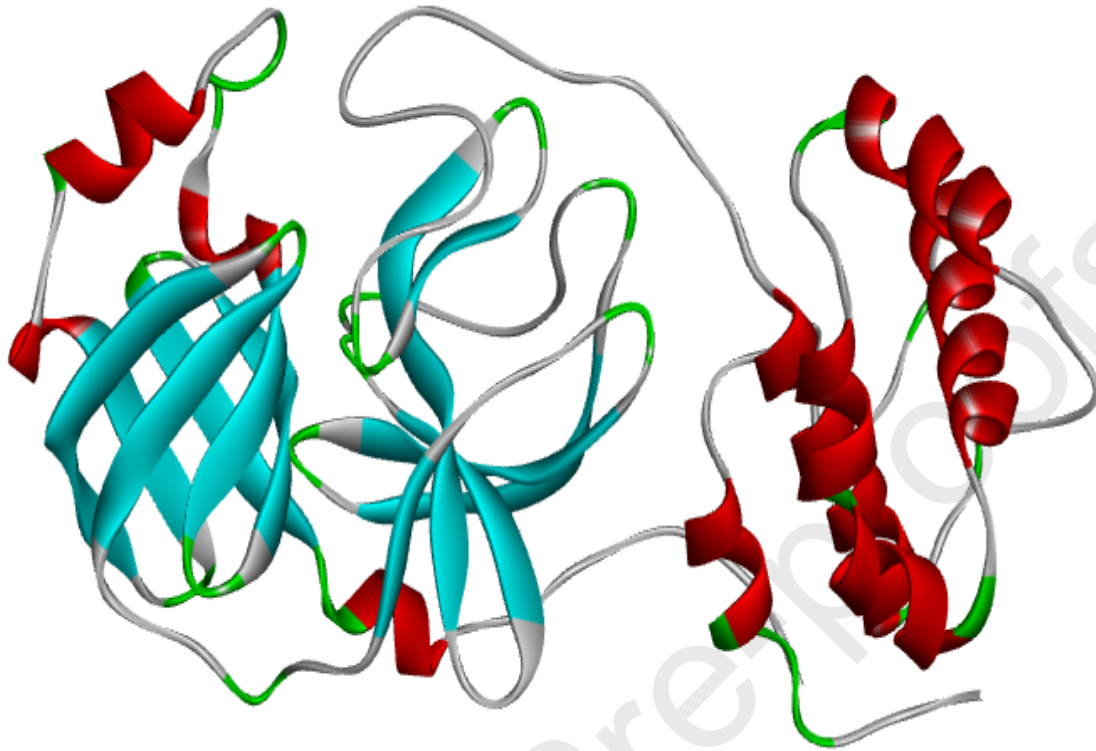
500 Waterhouse, A., Bertoni, M., Bienert, S., Studer, G., Tauriello, G., Gumienny, R., Heer, F.T., de
501 Beer, T.A.P., Rempfer, C., Bordoli, L., Lepore, R., Schwede, T., 2018. SWISS-MODEL:
502 homology modelling of protein structures and complexes. *Nucleic Acids Res*. 46, W296-W303.

503
504 Xu, Z., Peng, C., Shi, Y., Zhu, Z., Mu, K., Wang, X., Zhu, W., 2020. Nelfinavir was predicted to
505 be a potential inhibitor of 2019-nCov main protease by an integrative approach combining
506 homology modelling, molecular docking and binding free energy calculation. *bioRxiv*. doi:
507 <https://doi.org/10.1101/2020.01.27.921627>

508
509 Yin, Y., Wunderink, R.G., 2018. MERS, SARS and other coronaviruses as causes of pneumonia.
510 *Respirology*, 23, 130-137.

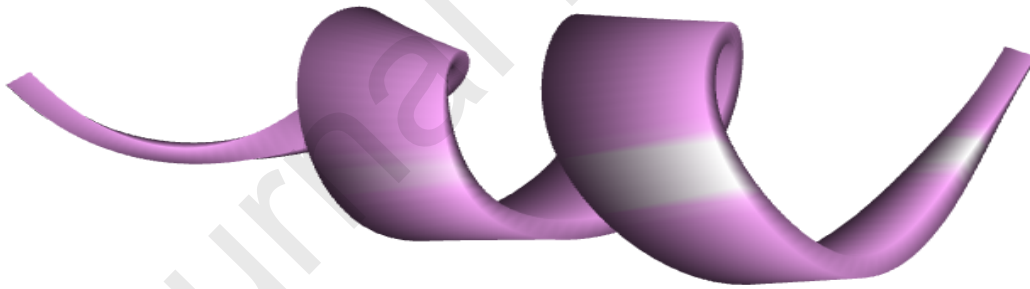
511
512

513
514



515
516

Figure 1: 3D structure of COVID-19 Protease (PDB ID: 6LU7)

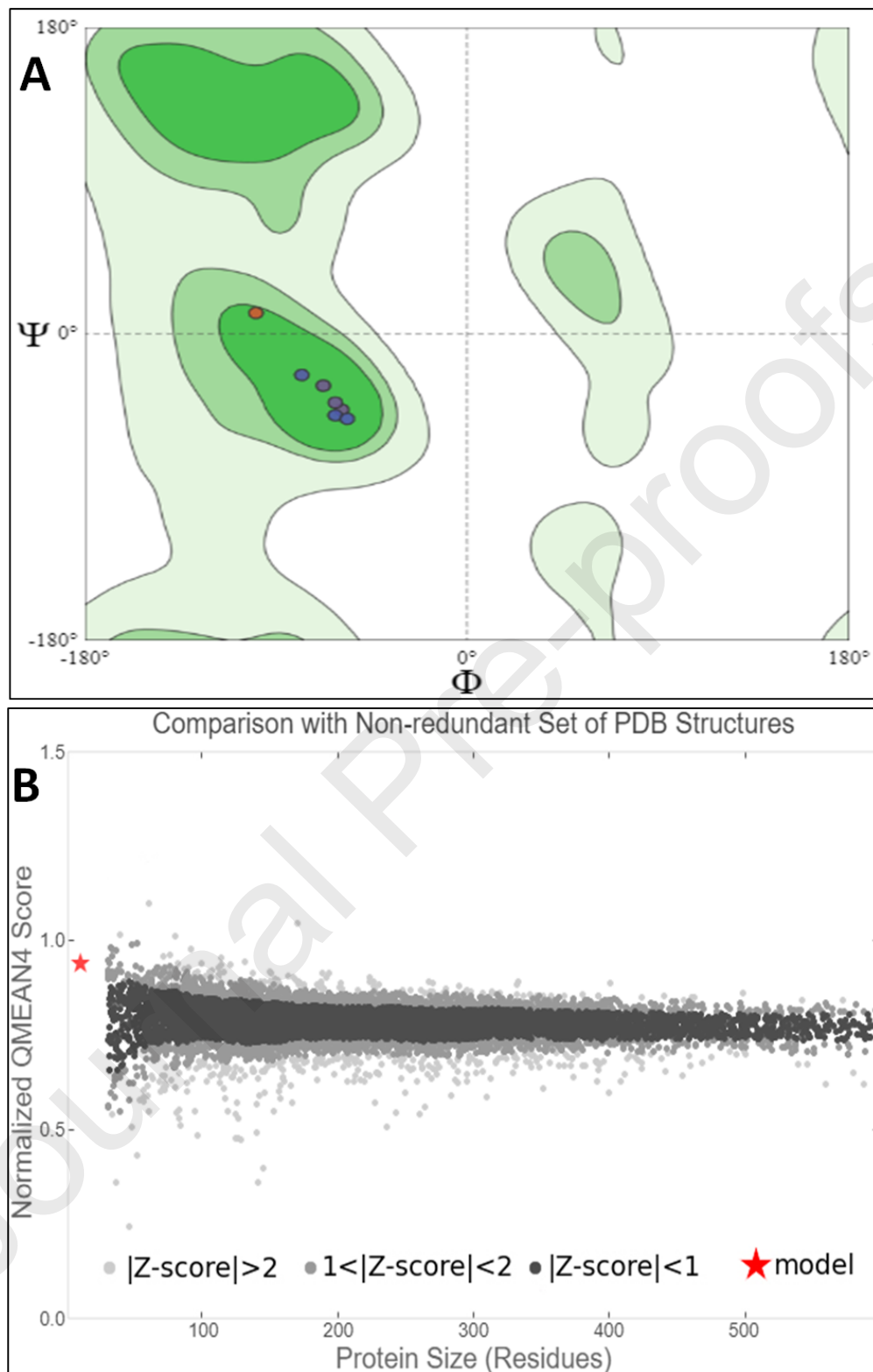


517
518

519

Figure 2: 3D structure of Modelled TAT-peptide

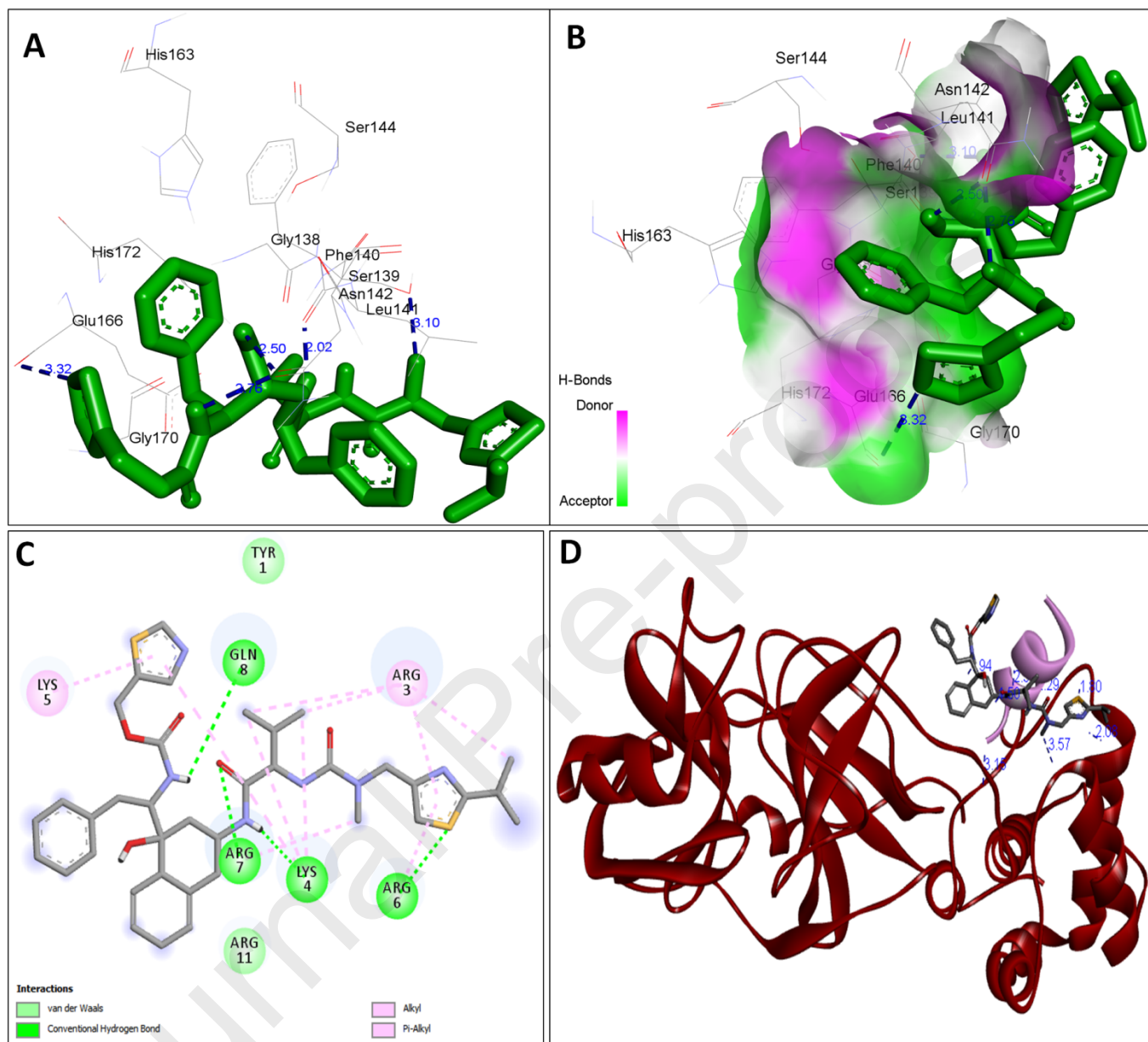
520



521

522 **Figure 3:** (A) Ramachandran Plot generated by MolProbity tool for the Modeled 3D TP validation. (B)
 523 Showing the modeled TP QMean4 Score and comparison with non-redundant set of PDB structures

524

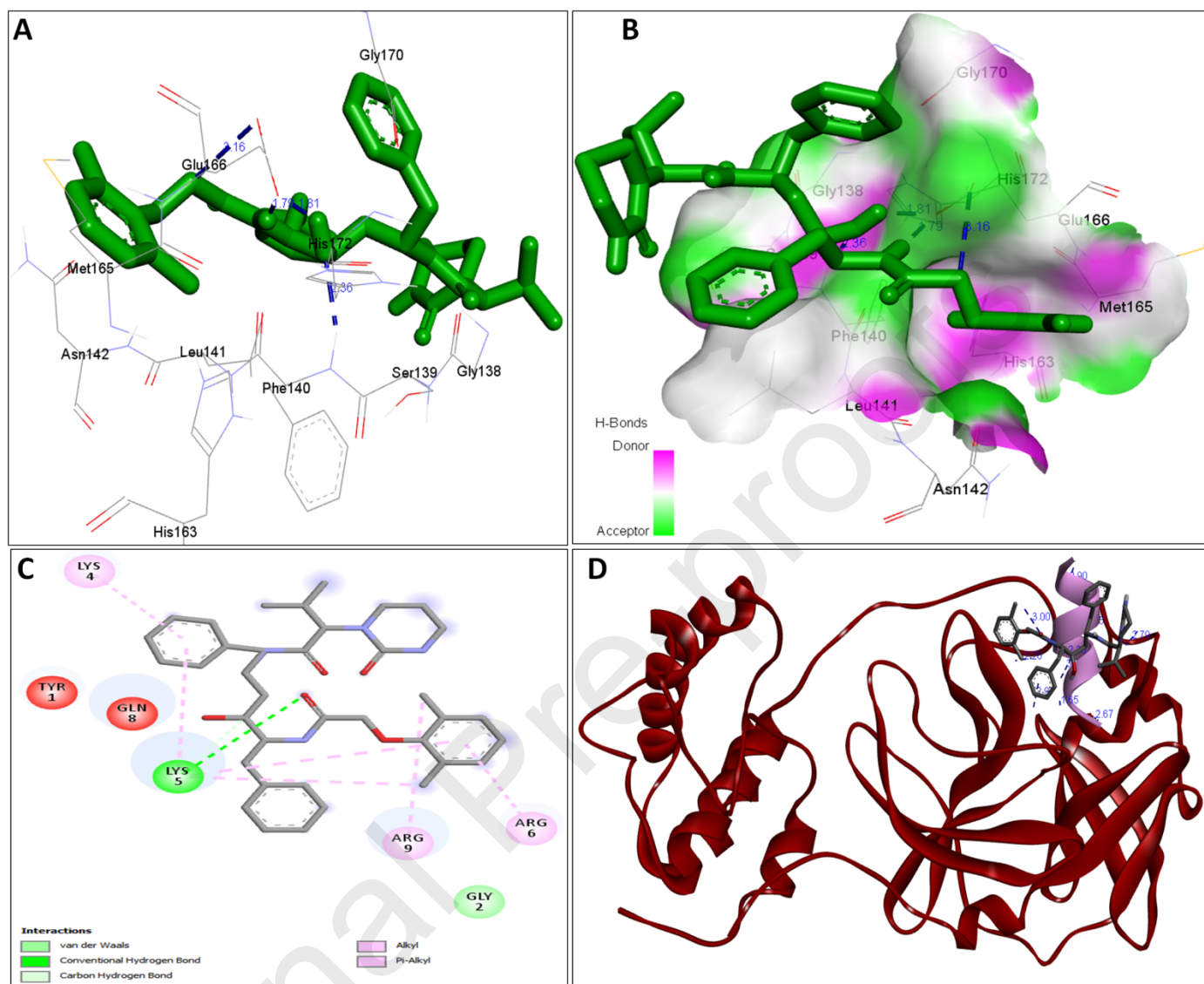


525

526 **Figure 4.** A: showing Ritonavir (green color stick pattern) interaction with COVID-19 Main
 527 protease (PDB ID: 6LU7) amino acid residues (grey color stick pattern) involved in hydrophobic
 528 interaction. Blue dotted lines represents hydrogen bonds; B: showing COVID-19 protease (PDB
 529 ID: 6LU7) pocket that accommodated the Ritonavir (green color stick pattern); C: 2D
 530 visualization of TP interaction with Ritonavir; D- showing TP (pink color ribbon pattern)
 531 conjugated Ritonavir complex (grey color stick pattern) interaction with COVID-19 protease (PDB
 532 ID: 6LU7) (maroon color ribbon pattern). Blue dotted lines are showing hydrogen bonds
 533 formation.

534

535



536

537 **Figure 5.** A: showing Lopinavir (green color stick pattern) interaction with COVID-19 Main
 538 protease (PDB ID: 6LU7) amino acid residues (grey color stick pattern) involved in hydrophobic
 539 interaction. Blue dotted lines represents hydrogen bonds; B: showing COVID-19 protease (PDB
 540 ID: 6LU7) pocket that accommodated the Lopinavir (green color stick pattern); C: 2D visualization
 541 of TP interaction with Lopinavir; D: showing TP (pink color ribbon pattern) conjugated Lopinavir
 542 complex (grey color stick pattern) interaction with COVID-19 protease (PDB ID: 6LU7) (maroon
 543 color ribbon pattern). Blue dotted lines are showing hydrogen bonds formation.

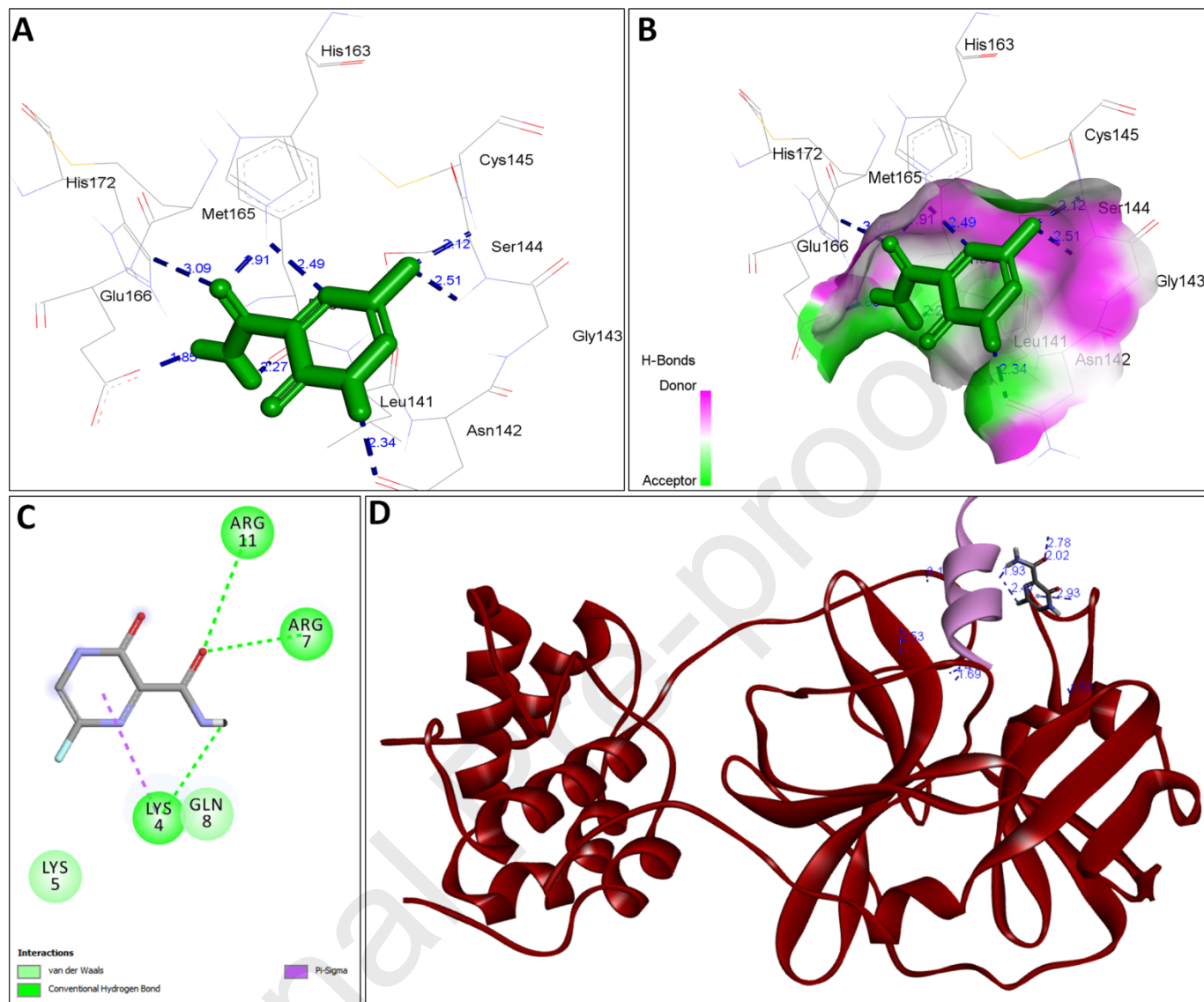
544

545

546

547

548



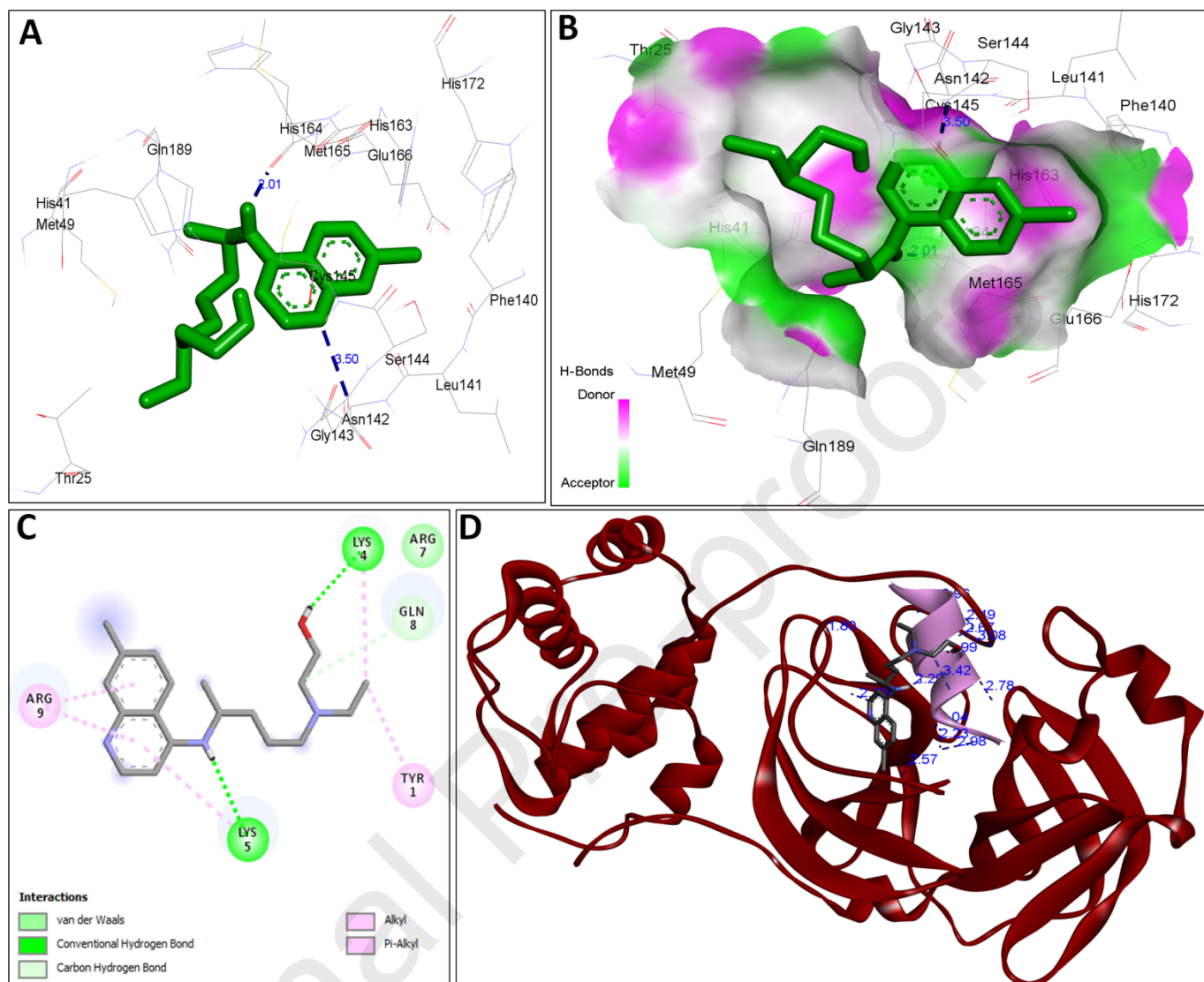
549

550

551 **Figure 6.** A: showing Favipiravir (green color stick pattern) interaction with COVID-19 Main
 552 protease (PDB ID: 6LU7) amino acid residues (grey color stick pattern) involved in hydrophobic
 553 interaction. Blue dotted lines represents hydrogen bonds; B: showing COVID-19 protease (PDB
 554 ID: 6LU7) pocket that accommodated the Favipiravir (green color stick pattern); C: 2D
 555 visualization of TP interaction with Favipiravir; D: showing TP (pink color ribbon pattern)
 556 conjugated Favipiravir complex (grey color stick pattern) interaction with COVID-19 protease
 557 (PDB ID: 6LU7) (maroon color ribbon pattern). Blue dotted lines are showing hydrogen bonds
 558 formation.

559

560



561
 562 **Figure 7.** A: showing hydroxychloroquine (green color stick pattern) interaction with COVID-19
 563 Main protease (PDB ID: 6LU7) amino acid residues (grey color stick pattern) involved in
 564 hydrophobic interaction. Blue dotted lines represents hydrogen bonds; B: showing COVID-19
 565 protease (PDB ID: 6LU7) pocket that accommodated the hydroxychloroquine (green color stick
 566 pattern); D: 2D visualization of TP interaction with hydroxychloroquine; D: showing TP (pink
 567 color ribbon pattern) conjugated hydroxychloroquine complex (grey color stick pattern)
 568 interaction with COVID-19 protease (PDB ID: 6LU7) (maroon color ribbon pattern). Blue dotted
 569 lines are showing hydrogen bonds formation.

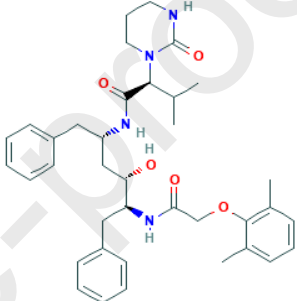
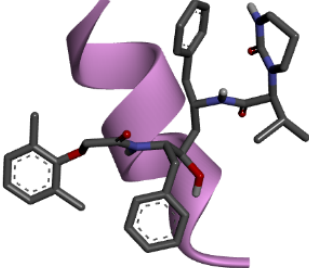
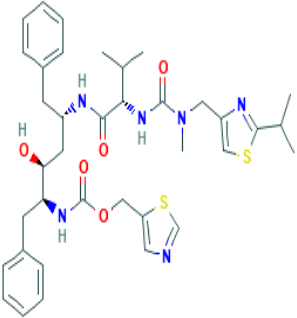
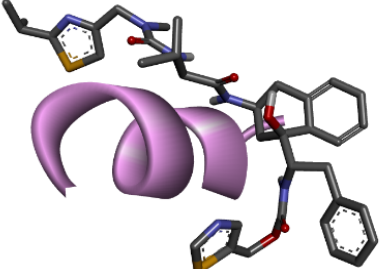

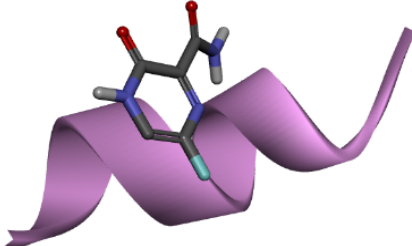
570

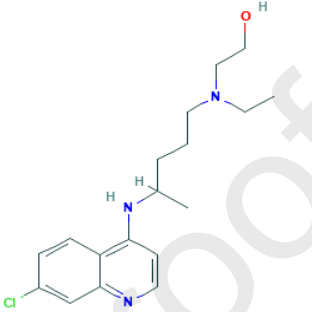
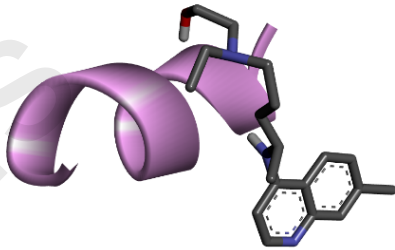
571

572

573

Table 1. Physiochemical description of 2D structure of repurposing drug molecules and 3D structure of TAT-peptide conjugated drugs used for molecular docking analysis with SARS-CoV-2 main protease (3CLpro)

S.No	Drugs	Molecular formula	Molecular weight	Canonical SMILES IDs	2D structure of drugs	3D structure of TAT-peptide conjugated drugs
1.	Lopinavir	C ₃₇ H ₄₈ N ₄ O ₅	628.8 g/mol	<chem>CC1=C(C(=CC=C1)C)OCC(=O)NC(CC2=CC=CC=C2)C(CC(CC3=CC=CC=C3)NC(=O)C(C(C)C)N4CCCNC4=O)O</chem>		
2.	Ritonavir	C ₃₇ H ₄₈ N ₆ O ₅ S ₂	720.9 g/mol	<chem>CC(C)C1=NC(=CS1)CN(C)C(=O)NC(C(C)C)C(=O)NC(CC2=CC=CC=C2)CC(C(CC3=CC=CC=C3)NC(=O)OCC4=CN=CS4)O</chem>		
3.	Favipiravir	C ₅ H ₄ FN ₃ O ₂	157.1 g/mol	<chem>C1=C(N=C(C(=O)N1)C(=O)N)F</chem>		

4.	Hydroxychloroquine	$C_{18}H_{26}ClN_3O$	335.8 g/mol	<chem>CCN(CCCC(C)NC1=C2C=CC(=CC2=NC=C1)Cl)CCO</chem>	 <p>The image shows the 2D chemical structure of Hydroxychloroquine. It consists of a quinoline ring system with a chlorine atom at the 7-position and a hydroxyethylamino group at the 4-position. The hydroxyethylamino group is further substituted with a butyl chain, which is in turn substituted with a hydroxyethylamino group.</p>	 <p>The image shows a 3D ribbon diagram of the Hydroxychloroquine molecule. The quinoline ring system is shown in a dark grey/black color, while the hydroxyethylamino group and its substituents are shown in a light purple color. The molecule is oriented in a way that shows its overall shape and the relative positions of the different parts.</p>
----	--------------------	----------------------	-------------	--	--	---

Journal Pre-proofs